

Supplemental Information

Microscopy and Tunable Resistive Pulse Sensing Characterization of the Swelling of pH-Responsive, Polymeric Expansile Nanoparticles

Aaron H. Colby,^a Yolonda L. Colson,^b and Mark W. Grinstaff^{a*}

a. Departments of Biomedical Engineering and Chemistry, Metcalf Center for Science and Engineering, Boston University, Boston, MA 02215

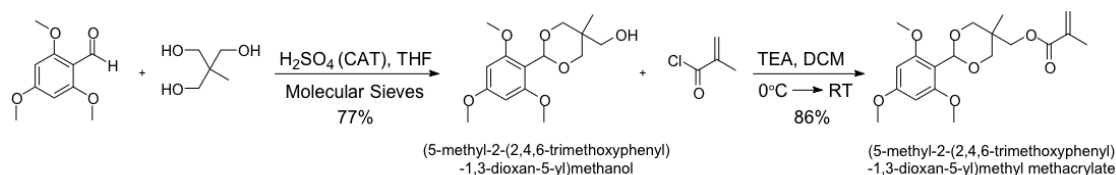
b. Division of Thoracic Surgery, Department of Surgery, Brigham and Women's Hospital, Boston, MA 02215

* Corresponding author: mgrin@bu.edu

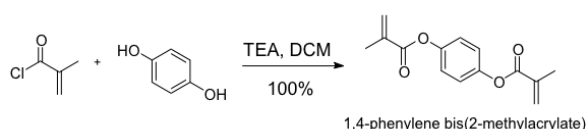
General Procedures and Materials

All chemicals were purchased from Sigma-Aldrich or Lancaster Synthesis and used without further purification unless otherwise stated. All reactions were performed under nitrogen atmosphere unless otherwise stated.

Monomer Synthesis



Crosslinker Synthesis



Iodine-Monomer Synthesis

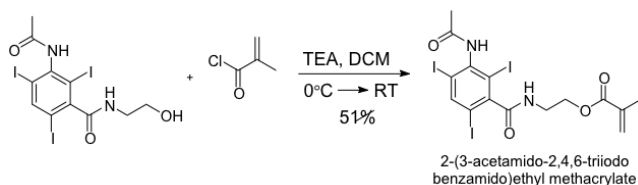


Figure S1. Synthesis schematic of the eNP monomer, (5-methyl-2-(2,4,6-trimethoxyphenyl)-1,3-dioxan-5-yl)methyl methacrylate, and crosslinker, 1,4-phenylene bis(2-methylacrylate), as well as iodinated monomer 2-(3-acetamido-2,4,6-triiodobenzamido)ethyl methacrylate.

Synthesis of (5-methyl-2-(2,4,6-trimethoxyphenyl)-1,3-dioxan-5-yl)methanol

The synthesis of this precursor compound follows a previously reported method with slight modifications to improve yield and purity.¹ First, 1,1,1-tris(hydroxymethyl)ethane (5.5115 g, 45.8 mmol, 3.0 equiv.) and 2,4,6-trimethoxybenzaldehyde (3.0 g, 15.291 mmol, 1.0 equiv.) were dissolved in 150 mL of tetrahydrofuran and 46.5 g of 5 Å molecular sieves were added as a desiccant. A catalytic amount of sulfuric acid was then added and the reaction mixture was shaken overnight at room temperature. When the reaction was complete, 6 mL triethylamine was added to neutralize the acid, followed by the addition of 100 mL of CH₂Cl₂. The molecular sieves were then removed using vacuum filtration. The solvent was removed via rotary evaporation under reduced pressure and the residue was dissolved in 75 mL of CH₂Cl₂. This mixture was then washed three times with 100 mM pH 8.0 Tris buffer and dried over anhydrous sodium sulfate. The solvent was subsequently removed using rotary evaporation under reduced pressure to give 3.282 g (77%) of (5-methyl-2-(2,4,6-trimethoxyphenyl)-1,3-dioxan-5-yl)methanol as a light yellow solid.

Synthesis of (5-methyl-2-(2,4,6-trimethoxyphenyl)-1,3-dioxan-5-yl)methyl methacrylate

The precursor, (5-methyl-2-(2,4,6-trimethoxyphenyl)-1,3-dioxan-5-yl)methanol (1.5 g, 5.028 mmol, 1.0 equiv.), and triethylamine (2.1 mL, 1.527 g, 15.084 mmol, 3.0 equiv.) were dissolved in 50 mL of CH₂Cl₂ and chilled to 0 °C. Methacryloyl chloride (1.08 mL, 1.157 g, 11.062 mmol, 2.2 equiv.) was then added drop wise to the solution while stirring. The reaction mixture was allowed to warm to room temperature while stirring overnight. Methanol (1 mL) was added to quench the remaining acid chloride. The mixture was then washed three times with 100 mM pH 8.0 Tris buffer and dried over anhydrous sodium sulfate. The solvent was subsequently removed using rotary evaporation under reduced pressure, and the product was purified by silica gel chromatography using 8:2 hexanes:ethyl acetate to give 1.547 g (86%) of (5-methyl-2-(2,4,6-trimethoxyphenyl)-1,3-dioxan-5-yl)methyl methacrylate as a white solid.

Synthesis of 1,4-phenylene bis(2-methylacrylate)

Hydroquinone (1.0 g, 9.09 mmol, 1.0 equiv.) and triethylamine (4.68 mL, 3.4 g, 3.33 mmol, 3.7 equiv.) were dissolved in 75 mL of CH₂Cl₂ and chilled to 0 °C. Methacryloyl chloride (3.28 mL, 3.52 g, 3.33 mmol, 3.7 equiv.) was then added drop wise to the solution while stirring. The reaction mixture was allowed to warm to room temperature while stirring overnight. 1 mL methanol was added to quench the remaining acid chloride. The mixture was then washed three times with 1 M NaOH, once with brine, and dried over anhydrous sodium sulfate. The solvent was subsequently removed using rotary evaporation under reduced pressure, and the product was purified by silica gel chromatography using 10:1 hexanes:ethyl acetate to give 2.24 g (100%) of 1,4-phenylene bis(2-methylacrylate) as a white solid.

Synthesis of 2-(3-acetamido-2,4,6-triiodobenzamido)ethyl methacrylate

The precursor, 3-acetamido-N-(2-hydroxyethyl)-2,4,6-triiodobenzamide (0.5 g, .833 mmol, 1.0 equiv.), and triethylamine (0.348 mL, 0.253 g, 2.399 mmol, 3.0 equiv.) were dissolved in 50 mL of CH₂Cl₂ and chilled to 0 °C. Methacryloyl chloride (0.179 mL, 0.192 g, 1.833 mmol, 2.2 equiv.) was then added drop wise to the solution while stirring. The

reaction mixture was allowed to warm to room temperature while stirring overnight. Methanol 1 mL was added to quench the remaining acid chloride. The mixture was washed three times with 100 mM pH 8.0 Tris buffer and then dried over anhydrous sodium sulfate. The solvent was subsequently removed using rotary evaporation under reduced pressure, and the product was purified by silica gel chromatography using 8:2 hexanes:ethyl acetate to give 0.315 g (51%) of 2-(3-acetamido-2,4,6-triiodobenzamido)ethyl methacrylate as a white solid.

Synthesis of Expansile Nanoparticles (eNPs)

Nanoparticles were prepared using a previously reported method.¹ Briefly, 50 mg of monomer, (5-methyl-2-(2,4,6-trimethoxyphenyl)-1,3-dioxan-5-yl)methyl methacrylate, and 0.5 mg of crosslinker, 1,4-phenylene bis(2-methylacrylate), were dissolved in 0.5 mL of CH₂Cl₂. This organic solution was then added to 2 mL of a 10 mM aqueous buffer solution containing 8 mg sodium dodecyl sulfate (SDS). This mixture was sonicated for 10 min (1 s pulses with a 2 s delay) with 20 W of power under an argon blanket to create the miniemulsion. When using the photochemical initiation method, following sonication, 20 μL of a 20 mM aqueous eosin Y solution and 4.27 μL of a 10% w/w aqueous 1-vinyl-2-pyrrolidinone solution were added to the emulsion. The mixture was then exposed to unfiltered light from a xenon arc lamp at 300 W for 20 min while stirring to initiate polymerization. Alternatively, when using the base-catalyzed reaction, following sonication, 20 μL of a 200 mM aqueous ammonium persulfate (APS) solution and 2 μL of N,N,N',N'-tetramethylethylenediamine (TEMED) were added to the emulsion and stirred under an argon blanket for 2 hrs. Alternatively, polymerization was conducted by adding 0.5 mg (1% wt/wt) azobisisobutyronitrile (AIBN) to the mixture prior to sonication and then, following sonication, heating the emulsion at 60 degrees Celsius for two hours. Following polymerization using any of these three methods, the suspension was then stirred overnight while open to the atmosphere to allow the remaining solvent to evaporate. The resulting polymeric nanoparticles were then dialyzed against 5 mM pH 7.4 phosphate buffer over 1 day to remove excess surfactant and salts. When synthesizing rhodamine-labeled nanoparticles, 0.1 mg of PolyFluor™ 570 (methacryloxyethyl tricarbonyl rhodamine B, Polysciences, Inc.) was dissolved in the CH₂Cl₂ along with the monomer and crosslinker before addition of the organic phase to the aqueous phase. When synthesizing acrylic pryene-labeled nanoparticles, 1 mg of PolyFluor™ 394 (1-pyrenylmethyl methacrylate, Polysciences, Inc.) was dissolved in the CH₂Cl₂ along with the monomer and crosslinker before addition of the organic phase to the aqueous phase. When synthesizing acrylic iodine-labeled nanoparticles, 1 mg of 2-(3-acetamido-2,4,6-triiodobenzamido)ethyl methacrylate was dissolved in the CH₂Cl₂ along with the monomer and crosslinker before addition of the organic phase to the aqueous phase.

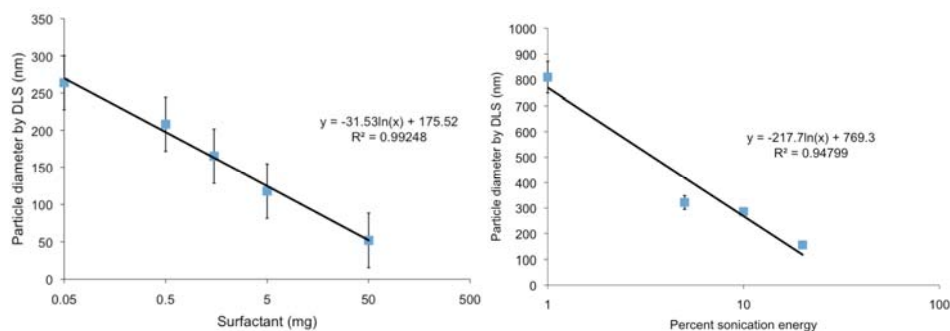


Figure S2. Nanoparticle size, as measured by DLS, is controlled by: **a)** the relative ratio of surfactant to monomer used in the mini-emulsion polymerization—in each case the mass of monomer used is 50 mg, and **b)** the sonication energy used to create the mini-emulsion.

Dynamic Light Scattering

A 10 μL aliquot of nanoparticle suspension was diluted in 3.0 mL of de-ionized water. The diameter of the nanoparticles was then measured using a Brookhaven Instruments, Inc. 90Plus particle-sizing instrument. All measurements were performed in triplicate.

Scanning Electron Microscopy

Scanning electron microscopy (SEM) was performed using a Zeiss SUPRA 55VP field emission SEM. Samples were prepared by diluting a small amount of nanoparticle suspension 1:100,000 in de-ionized water and then placing a drop of the diluted suspension on a silicon wafer. The sample was allowed to air-dry overnight and was then affixed to an aluminum sample stub using copper tape. The samples were coated with 5 nm of Au/Pd prior to imaging and were imaged at an accelerating voltage of 2 kV. Particle diameters were calculated from SEM micrographs using NIH ImageJ.

Freeze Fracture Transmission Electron Microscopy

For freeze-fracture transmission electron microscopy (ff-TEM), samples were quenched using a sandwich technique and liquid nitrogen-cooled propane. Using this technique a cooling rate of 10,000 Kelvin per second was reached avoiding ice crystal formation and artifacts possibly caused by the cryofixation process. The cryo-fixed samples were stored in liquid nitrogen for less than 2 hours before processing. The fracturing process was carried out in JEOL JED-9000 freeze-etching equipment and the exposed fracture planes were shadowed with Pt for 30 sec at an angle of 25-35 degrees and with carbon for 35 sec (2kV/60-70 mA, 1×10^{-5} Torr). The replicas produced this way were cleaned with concentrated, fuming HNO_3 for 1 day followed by repeated agitation with fresh chloroform/methanol (1:1 by vol.) at least 5 times. Replicas cleaned this way were imaged using a JEOL 100 CX electron microscope.

Transmission Electron Microscopy

Transmission electron microscopy (TEM) was performed on covalently iodine-labeled eNPs

using a JEOL 100 CX electron microscope. Samples were prepared by diluting a small amount of nanoparticle suspension 1:10 in de-ionized water with 1% wt/wt sodium dodecyl sulfate. A 5 μ L drop of the diluted suspension was then adsorbed to a carbon-coated grid that had been made hydrophilic by a 30 s exposure to a glow discharge. Excess liquid was removed with filter paper (Whatman #1) and the samples were stained with 0.75% uranyl formate for 30 s. After removing the excess uranyl formate with a filter paper, the grids were examined in a JEOL 1200EX Transmission electron microscope or a TecnaiG2 Spirit BioTWIN and images were recorded with an AMT 2k CCD camera.

Fluorescence Microscopy

Fluorescence microscopy was used to visualize the swelling of rhodamine-labeled eNPs. Covalently tagged rhodamine-eNPs were prepared as described above with an average diameter of 450 nm. Nanoparticles were diluted 1:1000 in either 10 mM pH 7.4 phosphate buffer or 10 mM pH 5.0 acetate buffer; both buffers contained 0.4% TWEEN. After allowing the particles to swell for 1 day, particles were viewed for counting and diameter determination using an inverted microscope with fluorescence epi-illumination from a Coherent Sapphire solid-state 488-nm laser. A 100X/1.40 NA oil immersion objective with Semrock long-pass filters was used to eliminate scattered light from the laser illumination and an Andor iXon 897 back-illuminated Electron-Multiplying CCD camera was used to record the images. Particle diameters were calculated from the SEM micrographs using NIH ImageJ.

qNano Measurements

qNano measurements were performed according to standard operating procedures. Briefly, a nanopore membrane is placed onto the pins of the qNano and stretched to a pin-to-pin width of 47 mm – 49 mm. Electrolyte is then added to the upper and lower fluid cell chambers created/separated by the nanopore membrane. The pore is cycled three or more times through stretching and un-stretching (~49 mm and ~44 mm, respectively) to remove hysteresis. Having opened the pore a voltage is applied across the membrane to establish a baseline electrical current through the pore. Fluid is then removed from the upper cell and replaced by a suspension of unknown particles. The diameter of the pore is adjusted until particles (visualized as individual blockades or “spikes” in the current trace) translocate the pore easily. If particles are too large or small to be seen on a given nanopore (i.e. they will not fit through the pore or do not cause a decrease in basal current greater than the background noise, respectively), a larger or smaller pore is substituted.

The magnitude of individual blockade events is related to the size of particles translocating the pore while particle concentration is related to the rate at which particles pass through the pore. The *relative* size and concentration of two different suspensions of particles is determined by comparing the peak height (i.e. blockade magnitude) and rate of translocation (particles/min). In order to determine *absolute* particle size of an unknown sample, the sample is measured, followed by measurement of a particle standard of known size. Comparison of the blockade magnitude between unknown and standard particles allows extrapolation of the unknown particles' size. It is essential, for the calibration to be correct, that both the standard and unknown sample are measured on the same pore, using the same applied voltage, pore stretch, and applied pressure/vacuum. Furthermore, using calibration

particles similar to the diameter and concentration of the unknown sample can facilitate the accuracy and ease of calibration.

To determine *absolute* particle concentration, both the unknown and calibration particles are measured at several different applied pressures. A linear plot of pressure vs. translocation rate is then constructed for each sample. Particle concentration is directly related to the slope of this curve. By taking the ratios of the slopes of the pressure vs. translocation rate graph for the unknown and calibration samples, the concentration of the calibration sample is used to determine the concentration of the unknown sample.

The following sections detail the particle dilutions and operating parameters (pore type/size, stretch, electrolyte buffer, applied pressures and voltage) used in qNano measurements. All calibrations were performed using NIST certified carboxylated polystyrene particles obtained through Izon Ltd. The nanopores and their diameter/stretch were chosen because these parameters allowed facile measurement of eNPs (either swollen or unswollen) and standards i.e. particles were able to readily translocate the pore without blocking, clogging, etc.

qNano was used to characterize eNP size as a function of swelling time at neutral and mildly acidic pH. To measure the size change after three days, eNPs were diluted 1:100 in pH 5.0 acetate buffer (10 mM) and pH 7.4 phosphate buffer (10 mM) on day 0; both buffers were modified with NaCl (25 mM) to increase buffer conductivity. After 3 days, particles maintained at pH 7.4 were further diluted 1:1000 in pH 7.4 buffer and sized on an NP200 nanopore at a stretch of 44 mm with an applied voltage of 0.3 V under atmospheric pressure. Particles maintained at pH 5.0 were further diluted in 1:1000 in pH 5.0 buffer and sized on an NP400 nanopore at a stretch of 46 mm with an applied voltage of 0.3 V under atmospheric pressure.

Time course measurements of eNPs maintained at pH 5.0 and pH 7.4 for 0, 3, and 5 days were conducted similarly to the above protocols. However, at each time point, particle size was measured on both a small NP400 and a large NP800 nanopore to ensure screening of the entire population. At each time point, particle size and count rate were measured under at least three different applied pressures on each nanopore thereby allowing accurate extrapolation of the measured particle concentration according to Izon protocols, and as detailed above.² The nanopore stretches, applied voltages, and pressures used at each time point and on each nanopore are given in Table S1.

To investigate the deformability of eNPs in their swollen state, eNPs were maintained at pH 5.0 and pH 7.4 for 3 days as described above. Particles in pH 5.0 buffer were then run on an NP800 nanopore at a stretch of 49 mm. Having sized a number of particles in this manner, the pore was then dynamically closed down until translocation events were observed to significantly increase in duration (pore stretch ranged from ~46 mm – 47 mm). Particles maintained at pH 7.4 were too small to be measured on an NP 800 nanopore and were therefore measured on an NP 400 nanopore at a stretch of 47 mm. Pore size was dynamically closed down to capture any particle behavior similar to that seen in eNPs at pH 5.0.

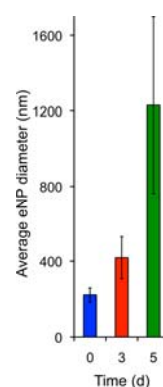


Figure S3. Average eNP diameter increases with swelling time at pH 5.0.

Day	Small Pore, NP400			Large Pore, NP800		
	macroscopic stretch (mm)	applied voltage (V)	applied pressure (cm H ₂ O)	macroscopic stretch (mm)	applied voltage (V)	applied pressure (cm H ₂ O)
0	44.29	0.90	3, 6, 9	48.14	0.48	3, 6, 9
3	45.44	0.90	3, 6, 9	48.14	0.48	3, 6, 9
5	45.44	0.90	3, 6, 9	48.14	0.48	3, 6, 9

Table S1. qNano parameters used to measure the time course size and concentration distribution of eNPs maintained at pH 5.0 and pH 7.4 for 0, 3, and 5 days.

Pyrene-eNPs To Measure eNP Hydrophobicity

Covalently encapsulated pyrene-labeled eNPs (Pyrene-eNPs) were synthesized as described above. Pyrene-eNPs were maintained in 10 mM pH 5.0 or pH 7.4 acetate or phosphate buffers for up to 3 days. Pyrene's emission spectrum was measured by exciting the particles at 339 nm using a Photon Technology International fluorimeter including an SC-500 shutter controller, MD-5020 motor driver, LPS-220B lamp power supply, and A-1010B arc lamp housing.

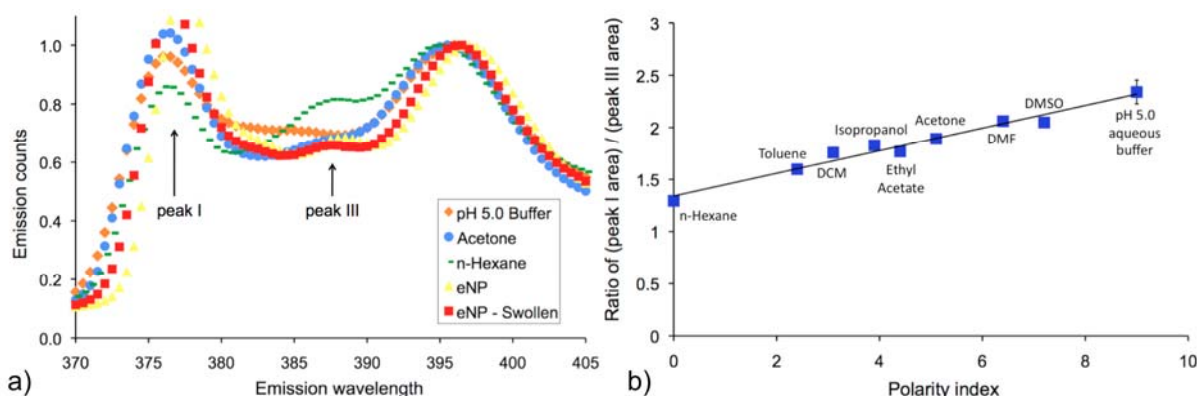


Figure S4. **a)** Normalized pyrene-methacrylate emission spectrum for pyrene in: pH 5.0 10 mM buffer (orange diamonds), acetone (blue circles), n-hexane (green dashes), and covalently encapsulated in unswollen (yellow triangles) and swollen (red squares) eNPs. **b)** Standard curve for (peak I area)/(peak III area) for pyrene-methacrylate v. polarity index of various solvents. (n = 3, mean ± SD)

1. A. P. Griset, J. Walpole, R. Liu, A. Gaffey, Y. L. Colson and M. W. Grinstaff, *J. Am. Chem. Soc.*, 2009, **131**, 2469-2471.
2. G. S. Roberts, S. Yu, Q. Zeng, L. C. L. Chan, W. Anderson, A. H. Colby, M. W. Grinstaff, S. Reid and R. Vogel, *Biosensors and Bioelectronics*, 2012, **31**, 17-25.